

Optical Transmission, Photoluminescence, and Raman Scattering of Porous SiC Prepared from *p*-Type 6H SiC

Sangsig KIM^{1,2,*}, Jonathan E. SPANIER² and Irving P. HERMAN²

¹Department of Electrical Engineering, Korea University, Seoul 136-701, Korea

²Department of Applied Physics, Columbia University, New York, New York 10027, U.S.A.

(Received February 18, 2000; accepted for publication July 26, 2000)

The optical transmission, temperature-dependence of the photoluminescence (PL), and Raman scattering of porous SiC prepared from *p*-type 6H-SiC are compared with those from bulk *p*-type 6H-SiC. While the transmission spectrum of bulk SiC at room temperature reveals a relatively sharp edge corresponding to its band gap at 3.03 eV, the transmission edge of porous SiC (PSC) is too wide to determine its band gap. It is believed that this wide edge might be due to surface states in PSC. At room temperature, the PL from PSC is 20 times stronger than that from bulk SiC. The PL PSC spectrum is essentially independent of temperature. The relative intensities of the Raman scattering peaks from PSC are largely independent of the polarization configuration, in contrast to those from bulk SiC, which suggests that the local order is fairly random.

KEYWORDS: porous, *p*-type 6H-SiC, optical transmission, photoluminescence, Raman scattering, surface states, polarization configuration

1. Introduction

Porous SiC (PSC) has been investigated recently because it is a potentially attractive material for fabricating UV light emitting diodes (LEDs),¹⁾ efficient photodetectors,²⁾ hydrocarbon gas sensors,³⁾ and as a novel substrate for epitaxy.⁴⁾ One reason for some of this interest is the much higher photoluminescence (PL) emission efficiency from PSC than that from bulk SiC.^{1,5–7)} The energy of the peak PL emission in PSC is below the band gap of the bulk SiC. If quantum confinement were important, as it may be in porous Si,^{5,6,8,10)} the PL energy would be above the band gap energy. While the origin of visible PL from porous Si has not been identified definitively, the differences in the PL from porous and bulk SiC might offer important insight into the origin of PL in porous semiconductors. This is examined here for PSC prepared from *p*-type SiC because of evidence of a possible high-energy peak near 3.7 eV observed in the cathodoluminescence of some *p*-type SiC samples.¹¹⁾

PSC prepared from *p*-type 6H SiC was studied by transmission, PL, and Raman scattering spectroscopies, each of which provides different information. Optical transmission can help determine the band gap. PL performed at different temperatures can give information on radiative and nonradiative mechanisms. Raman scattering can analyze the microcrystalline structure and reveal the degree of anisotropy in this structure. Reference measurements were made on bulk SiC.

2. Experimental Procedure

The PSC sample was prepared by dark-current anodization ($J = 5 \text{ mA/cm}^2$) of a single-crystal *p*-type 6H-SiC wafer ($N_A = 2 \times 10^{18}/\text{cm}^3$, Al acceptors; also with N donors) in aqueous HF.^{11–13)} The *c*-axis was within 3.5° of the normal to this wafer. The underlying SiC substrate was removed by raising the current density to $>500 \text{ mA/cm}^2$ for several minutes following the anodization, to get a free-standing PSC film that was approximately $150 \mu\text{m}$ thick. The average crystallite size was estimated to be 8 nm by transmission electron microscopy (TEM).^{12,13)} Part of the original wafer was used as the bulk SiC reference.

Transmission spectra of free-standing PSC and bulk SiC were taken at 300 K using a 75 W xenon lamp. PL from both samples was measured from 9 to 300 K in backscattering configuration with the 351-nm line from an Ar-ion laser (15 mW). The transmitted light and PL were dispersed by a 0.85-m double spectrometer and detected by a cooled GaAs photomultiplier. The absorption coefficient α was determined from 1.8 to 3.2 eV using the relation $\alpha = (1/d) \ln[T(\lambda)/T_0(\lambda)]^{-1}$, where T and T_0 are the measured transmittances with and without the sample, respectively, and d is the thickness of the sample.¹⁴⁾ The sample reflectance is assumed to be independent of wavelength λ . The PL spectra were corrected for variations in spectral sensitivity of the optical apparatus by using tungsten and xenon lamps for spectral calibration.

Unpolarized and polarized Raman scattering spectra of both samples were taken at room temperature in backscattering configuration using the 488-nm line from an Ar ion laser (10 mW), with an 0.6-m triple spectrometer for dispersion and a CCD detector for detection. The Raman mode identification and polarization configurations from ref. 15 were used here. In the *xy* plane, the x' axis makes a 45° angle to the x axis and y' is perpendicular to the x' axis. The dependence of the Raman spectra on the laser power was checked to make sure that the laser did not heat the sample. The Raman intensities increased linearly with laser power, and the Raman shifts and widths were independent of power. The resolution of the Raman spectra is better than 1 cm^{-1} .

3. Results

The normalized transmission spectrum of *p*-type bulk SiC at room temperature is shown in Fig. 1. This is converted into an absorption spectrum in Fig. 2. For doped, indirect-gap semiconductors, the absorption spectrum has the following spectral dependence:

$$\alpha(E) = AN_A(E - E_{BG} - \xi_p)^2 \quad (3.1)$$

where A is a constant, E_{BG} the band gap, and ξ_p the Burstein-Moss shift.¹⁵⁾ From the absorption spectrum in Fig. 2, the effective band gap ($E_{BG} + \xi_p$) of the bulk *p*-type SiC sample is 3.03 eV. The band gap of undoped 6H-SiC is known to be 2.86 eV at room temperature.^{5,6,16,17)} The 0.17 eV difference between these two values is believed to come from the

*E-mail address: sangsig@kucncx.korea.ac.kr

Burstein-Moss shift in this heavily doped sample.

PL spectra of bulk SiC at selected temperatures are shown in Fig. 3. At 9 K, a peak associated with donor-acceptor pairs (DAPs) around 2.65 eV is dominant and a very weak, broad emission tail is seen at the lower energies. The intensity of this peak decreases rapidly with increasing temperature. At 100 K it is 100 times weaker than at 9 K, and the DAP peak is not seen at and above 150 K. At and above 150 K there

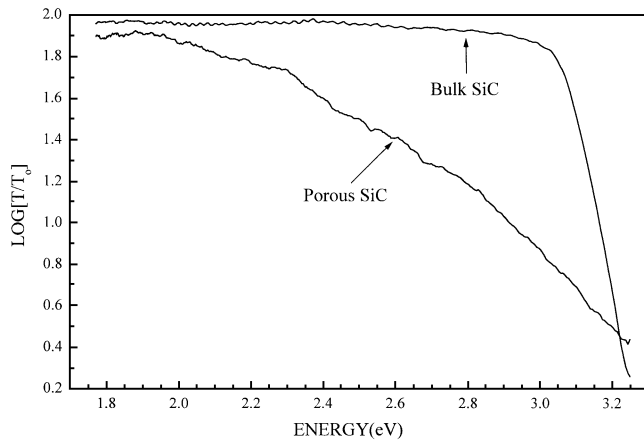


Fig. 1. Transmission spectra of porous and bulk SiC at room temperature.

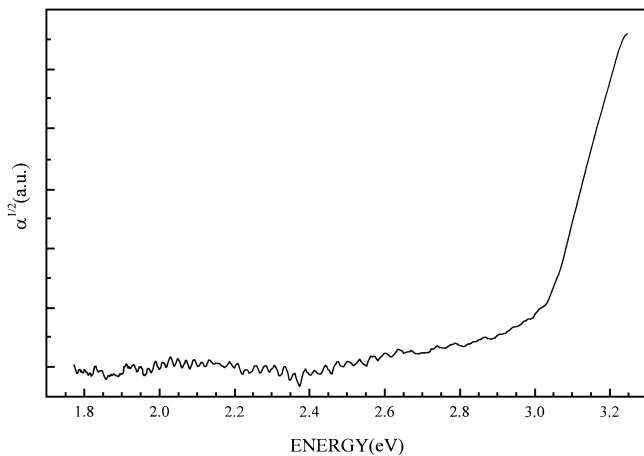


Fig. 2. Absorption spectrum of bulk SiC at room temperature.

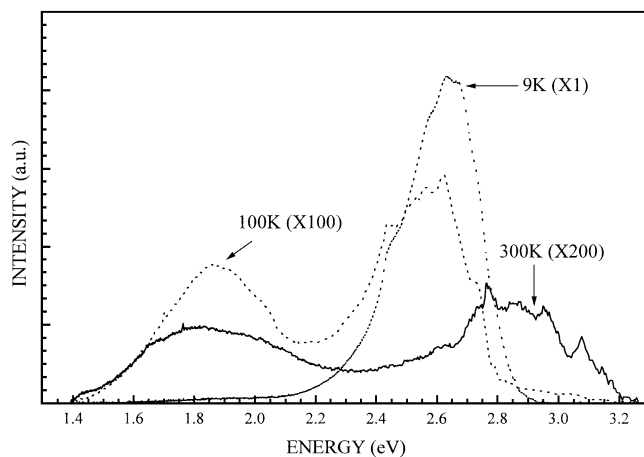


Fig. 3. PL spectrum of bulk SiC at selected temperatures, taken with 351-nm excitation.

is a dominant and broad emission near 1.9 eV, which is 200 times weaker than the DAP line at 9 K. [This feature appears to be independent of temperature (9–300 K), and is likely the same as the low energy tail at 9 K.] At and above 200 K, there is another broad and weaker emission near 2.9 eV. This latter feature decreases slowly with temperature.

Figure 4 shows that the Gaussian fitted peak energy (2.6 eV) and PL line width (0.8 eV) of *p*-PSC are essentially independent of temperature from 9 to 300 K. The integrated PL intensity varies little between 9 and 300 K. At 300 K, the

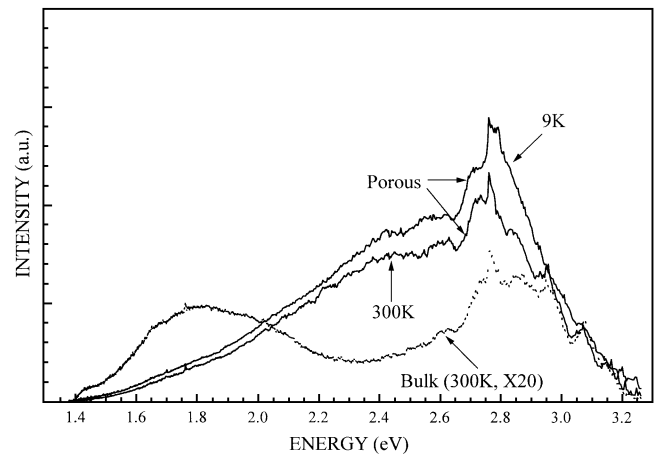


Fig. 4. PL spectrum of porous SiC at 9 and 300 K, taken with 351-nm excitation.

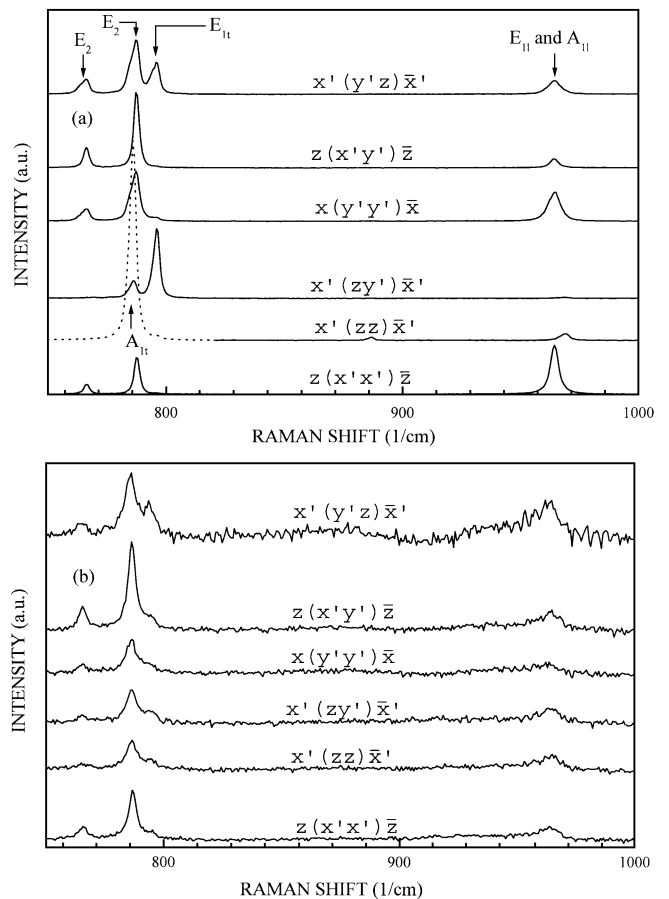


Fig. 5. Raman scattering spectra for (a) bulk SiC and (b) porous SiC for various polarization configurations at room temperature (488-nm excitation). The photoluminescence background has been subtracted in (b).

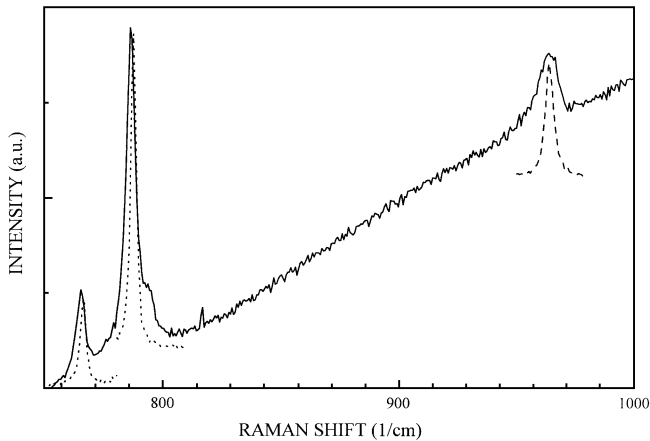


Fig. 6. Raman scattering spectra for bulk SiC and PSC in backscattering configuration at room temperature (488-nm excitation), with the photoluminescence background remaining. The dotted lines are the respective Raman peaks from bulk SiC.

integrated PL intensity from the porous sample is 20 times larger than that from the bulk sample. This enhanced PL efficiency has been seen in *p*-PSC⁷⁾ as well as *n*-PSC before.^{5,6)} The PL lineshape for energy >2.8 eV is similar for both porous and bulk SiC at 300 K.

PL is also seen in PSC using photons with energies below the band gap of bulk SiC. Such PL was seen at 488 nm (2.54 eV) and 647 nm (1.92 eV) in PSC, but not in bulk SiC. As the photon energy is decreased, the high energy tail vanishes and the peak shifts to lower energy [to ~ 2.0 eV (620 nm) for 488 nm excitation and to ~ 1.8 eV (700 nm) for 647 nm].

Figures 5(a) and 5(b) show the Raman spectra of the crystalline and porous SiC for several polarization configurations. The large luminescence background that is present in each PSC spectrum, even using “below band gap” light, has been subtracted using a quadratic fit. Figure 6 shows a spectrum taken in backscattering configuration with no polarization analyzer and with the PL background remaining.

4. Discussion

There is strong and broad absorption at energies lower than the effective band gap in PSC (Fig. 1). This below band gap absorption mimics the PL spectrum (Fig. 4). Since the PSC is crystalline, it is expected to be transparent for energies below the band gap. However, this observation suggests the presence of tail states in the band gap, as seen in amorphous semiconductors,^{5,6,12,13)} which may be associated with surface states. One model of absorption in porous Si involves a continuum of band gap energies (above the gap of the crystal) determined by quantum confinement and the crystallite size distribution.¹⁸⁾ For our PSC sample, the average crystallite size is 8 nm.^{12,13)} While a continuum of the band gap states due to a distribution of crystallite sizes is also expected in PSC, the transmission spectrum does not give any evidence of this. It may be masked by the strong absorption below the crystalline band gap.

Using 351-nm excitation, PL from porous and bulk SiC at 300 K is strong at energies far below the band gap of the crystal determined above (3.03 eV); emission also appears to extend to energies somewhat higher than this band gap. The SiC band gap at 9 K is 0.05 eV larger than that at 300 K.

The Burstein-Moss shift should be negligible at 9 K, so the band gap should be 2.91 eV. At 9 K, the DAP peak (Fig. 3) is 0.3 eV below the band gap and its high-energy tail barely reaches the band gap. The PL emission from the PSC is independent of temperature, and that from the bulk sample is fairly independent of temperature above 200 K. This is unexpected since the band gap E_{BG} is known to decrease with temperature. This suggests that the PL emission from PSC seen near the band gap is not directly related to this gap, and may be related to deep states, perhaps the same that lead to PL at room temperature in bulk SiC.

At present, the origin of PL from room-temperature bulk SiC is also not clear. It has been associated with the D_1 defect center¹⁹⁾ and with DAP recombination.¹⁰⁾ Although the D_1 spectrum consists of very sharp zero-phonon lines around 2.6 eV and a number of phonon replicas at low temperature (as shown in ref. 20), there has been no definitive evidence that the broad PL emission at room temperature over the energy region of 1.4 to 3.2 eV is associated with the D_1 defect center. Neither the D_1 defect center or the DAP can explain the observation of the room temperature PL at energies above the band gap energy.

Raman scattering measurements can determine the local grain-like structure of materials (size; rod- or sphere-like shape), such as porous semiconductors, by examining the effect of the local confinement of phonons on the Raman shift and linewidth.^{21–23)} If multiple scattering is not severe, analysis of the Raman spectrum with different polarization configurations can determine how the local order deviates from that in material with perfect crystalline order.^{21–23)}

Figure 5(b) shows that the relative intensity of peak in the Raman scattering spectra from PSC are largely independent of polarization configuration, while those for bulk SiC [in Fig. 5(a)] are configuration dependent. This observation suggests that the porous structure of the PSC is highly random; i.e. the structure that remains after anodization is not merely a skeletal remnant of the crystal, but that the structure is locally rotated (randomly). Alternatively, the observation could also mean that there is much elastic scattering of incident and Raman scattered photons;^{21–23)} transmission experiments suggest that such elastic scattering is not that significant. There is also a weak peak just below the LO phonon in PSC (and not in bulk SiC). It is likely due to surface phonons which are expected to be observed in this material.²⁴⁾

The Raman scattering spectra from PSC in Fig. 5(b) (with the background PL removed) shows that the widths of the Raman peaks are only slightly broader and their positions are only slightly shifted relative to those of bulk SiC. Such broadening was also observed for *n*-type PSC.^{5,6)} Such broadening and peak shifting in the Raman spectra of the PSC could arise from two effects. Momentum conservation at Γ is relaxed due to finite-size effects. For porous Si, the broadening and red-shift relative to the Raman peak of bulk crystalline Si have been described by including finite-size confinement in nanocrystals.^{21–23)} Furthermore, for PSC the deviation of the local lattice structure from crystallinity could also strongly affect the Raman lineshape, since the intensities and positions of several of the active Raman modes of bulk SiC depend on the angle between the propagation vector and the *c*-axis. Hence, the second reason why the widths can broaden and the peaks shift in PSC can be that the crystalline selection rules

are relaxed due to the irregularity of the local lattice structure. For porous Si, the irregularity does not influence the Raman peak position since only the LO peak is active for bulk Si in backscattering geometry.

Finite-size effects are estimated for PSC by using the quantitative model for the Raman spectrum proposed for porous Si in ref. 21–23. In this model, the Brillouin zone is assumed to be spherically symmetric. For phonon modes in 6H-SiC, only the axial direction of the Brillouin zone needs to be considered.^{25,26} According to this model, the Raman spectrum $I(\omega)$ of spherical nanocrystals with diameter L is

$$I(\omega) \propto \int \exp(-q^2 L^2) \frac{d^3 q}{[\omega - \omega(q)]^2 + (\Gamma/2)^2} \quad (4.1)$$

where q is in units of $2\pi/c$ and L in units of c with $c = 1.5117$ nm being the lattice constant along the c -axis. The axial direction dispersion relations for optical phonons in 6H-SiC are well known^{25–27} so that the analytic forms of $\omega(q)$ for each mode can be obtained by fitting to the dispersion curves. This estimate for 8-nm-size particles predicts that E_2 (at 766 cm^{-1}) shifts toward larger Raman shifts by 2 cm^{-1} , E_2 (at 788 cm^{-1}) does not shift, and E_{1l} and A_{1l} shift down by 3 cm^{-1} . This is inconsistent with our observation that E_2 peaks (at 766 cm^{-1} and 788 cm^{-1}) shift toward lower energy by 2 cm^{-1} , and that the E_{1l} and A_{1l} peaks do not shift. Therefore, the observed shift of Raman peaks for PSC may not be primarily due to the relaxation of momentum conservation associated with finite-size effects. However, since these expected shifts are small for these relatively large “nanocrystals,” these difference may not be significant. Relatively small broadening is also predicted (and observed) for this material with relatively large local structures.

The line shape of the Raman spectrum from porous SiC may resemble the angle-averaged spectrum of bulk SiC under all possible configurations because of the irregularity of the local lattice structure. In the spectra of bulk SiC in Fig. 5(a) the relative strength of the peaks near 766 , 788 , 796 and 964 cm^{-1} depends on the polarization configuration, while for PSC [Fig. 5(b)] the relative intensities of the four peaks are largely independent of polarization configuration.

At present, we are not sure whether the quantitative model for the Raman spectrum $I(\omega)$ proposed for porous Si is not appropriate for PSC because the finite size effect may be too weak to be observed. Still, the mechanism of the broadening and shift should be different for PSC and porous Si, because the irregularity of the local lattice structure affects only polarization effects in porous Si, but, in addition, affects the observed Raman shifts and linewidths in PSC.

5. Concluding Remarks

The effective band gap of the bulk SiC is determined here as 3.03 eV , but a band gap for PSC can not be determined because of the wide absorption observed in the transmission spectrum. This absorption may be due to the presence of the surface states. PL from p -type PSC is 20 times stronger than that from bulk SiC. The states involved in the PL emission

from the PSC seen near the band gap might be related to those important in room temperature PL in the bulk SiC. The line shapes of polarized Raman scattering from PSC are largely independent of polarization configuration, which suggests that the local order of this porous structure is fairly random.

Acknowledgements

The authors acknowledge support from the Joint Services Electronics Program (JSEP) under Contract No. DAA-G-55-97-1-0166, the HANARO Program and Kulite Semiconductor Products, Inc., Leonia, NJ, U.S.A.

- 1) H. Mimura, T. Matsumoto and Y. Kanemitsu: *J. Non-Cryst. Solids* **198** (1996) 2.
- 2) K. H. Wu, Y. K. Fang, W. T. Hsieh, J. J. Ho, W. J. Lin and J. D. Hwang: *Electron. Lett.* **34** (1998) 2243.
- 3) V. B. Shields, M. A. Ryan, R. M. Williams, M. G. Spencer, D. M. Collins and D. Zhang: *Proc. IOP Conf. Silicon Carbide and Related Materials*, eds. S. Nakashima, H. Matsunami, S. Yoshida and H. Harima (IOP Publishing, Bristol, 1996) Inst. Phys. Conf. Ser., No. 142, Chap. 7, p. 1067.
- 4) J. E. Spanier, G. T. Dunne, L. B. Rowland and I. P. Herman: *Appl. Phys. Lett.* **76** (2000) 3879.
- 5) T. Matsumoto, J. Takahashi, T. Tamaki, T. Futagi, H. Mimura and Y. Kanemitsu: *Appl. Phys. Lett.* **64** (1994) 226.
- 6) H. Mimura, T. Matsumoto, J. Takahashi and Y. Kanemitsu: *Appl. Phys. Lett.* **65** (1994) 3350.
- 7) J. E. Spanier, G. S. Cargill III, I. P. Herman, S. Kim, D. R. Goldstein, A. D. Kurtz and B. Z. Weiss: *Mater. Res. Soc. Symp. Proc.* **452** (1997) 491.
- 8) S. S. Iyer and Y.-H. Xie: *Science* **260** (1993) 40.
- 9) C. Delerue, M. Lannoo, G. Allan and E. Martin: *Thin Solid Films* **255** (1995) 27.
- 10) V. Petrova-Koch, O. Sreseli, G. Polinski, D. Kovalev, T. Muschik and F. Koch: *Thin Solid Films* **255** (1995) 107.
- 11) J. S. Shor, I. Grimberg, B. Z. Weiss and A. D. Kurtz: *Appl. Phys. Lett.* **62** (1993) 2836.
- 12) J. S. Shor, L. Bemis, A. D. Kurtz, I. Grimberg, B. Z. Weiss, M. F. MacMillan and W. J. Choyke: *J. Appl. Phys.* **76** (1994) 4045.
- 13) A. M. Danishevskii, M. V. Zamoryanskaya, A. A. Sitnikova A. A., V. B. Shuman and A. A. Suvorova: *Semicond. Sci. Technol.* **13** (1998) 1111.
- 14) H. Teisseyre, P. Perlin, T. Suski, I. Grzegory, S. Porowski, J. Jun, A. Pietraszko and T. D. Moustakas: *J. Appl. Phys.* **76** (1994) 2429.
- 15) J. I. Pankove: *Optical Processes in Semiconductors* (Dover, New York, 1971) p. 39.
- 16) H. R. Philipp and E. A. Taft: *Silicon Carbide*, eds. J. R. O’Corner and J. Smiltens (Pergamon, London, 1960) p. 366.
- 17) R. P. Devaty and W. J. Choyke: *Phys. Status Solidi A* **162** (1997) 5.
- 18) G. Vincent, F. Leblanc, I. Sagnes, P. A. Badoz and A. Halimaoui: *J. Lumin.* **57** (1993) 217.
- 19) A. O. Konstantinov, A. Henry, C. I. Harris and E. Janzen: *Appl. Phys. Lett.* **66** (1995) 2250.
- 20) Ch. Haberstroh, R. Helbig and R. A. Stein: *J. Appl. Phys.* **76** (1994) 509.
- 21) Z. Sui, P. P. Leong, I. P. Herman, G. S. Higashi and H. Temkin: *Appl. Phys. Lett.* **60** (1992) 2086.
- 22) P. Deak, Z. Hajnal, M. Stutzmann and H. D. Fuchs: *Thin Solid Films* **255** (1995) 241.
- 23) I. Gregora, B. Champagnon, L. Saviot and Y. Monin: *Thin Solid Films* **255** (1995) 139.
- 24) J. E. Spanier and I. P. Herman: *Phys. Rev. B* **61** (2000) 10437.
- 25) D. W. Feldman, J. H. Parker, Jr., W. J. Choyke and L. Patrick: *Phys. Rev.* **170** (1968) 698.
- 26) G. Salvador and W. F. Sherman: *J. Mol. Struct.* **247** (1991) 373.
- 27) K. Goehlert, G. Irmer, L. Michalowsky and J. Monecke: *J. Mol. Struct.* **219** (1990) 135.